E877 Note # SUNYSB-CHANG-95-005

September 30, 1995

Event Shape of E_T Production With Respect to the Reaction Plane of 1993 $Au + Au$ data

Wen-Chen Chang

State University of New York, Stony Brook, NY 11794-3800

ABSTRACT

We perform Fourier analysis of transverse energy production with respect to the reaction plane for $Au + Au$ collision at 10.8 GeV per nucleon. The methods of how to correct the distorted reaction plane distribution and determine the reaction plane resolution are discussed and implemented in the analysis. Comparison of the results with the cascade model(RQMD) prediction and the approach without reaction plane determination are also shown.

1 Introduction

By fitting the distribution of Fourier moments of the transverse energy event shape with the modified Bessel function to locate the shift of the centroid, directed flow is conclusive in AGS[1]. The greatest advantage of this approach is that there is no need of input of reaction plane event by event, however the requirement of statistics for good fit limits the width of observing pseudo-rapidity window. The existence of flow signals in the calorimeters($TCAL$, $PCAL$) make it become possible to extract reaction plane information event by event from them. As a further step, we can take the more direct approach by determining reaction plane event by event and studying the event-averaged azimuthal E_T distribution with respect to the estimated reaction plane in some independent window. Then we need to correct the Fourier coefficients by the angular resolution in the determination of reaction plane[4] and demonstrate their values in different centrality and pseudo-rapidity bins.

The note is organized as follows. In the first section, the strategy of whole analysis is described. Then we discuss the methods of how to determine reaction plane resolution. Finally we present results of the analysis of 1993 $Au + Au$ data and end with a summary.

2 Strategy of Analysis

The reaction plane is defined as the plane extended by two vectors, impact parameter $\vec{b}$ and beam momentum $\vec{P}$. The direction of reaction plane in the transverse plane is called $directivity(\vec{D})$ and can be estimated in the detector(or part of it) with full 2π azimuthal coverage by adding all unit azimuthal vector of each cell weighted by chosen measured variables(like $E_T, \vec{P}$) or some constant(like multiplicity).

In our experiment, by utilizing the upstream calorimeters ($PCAL$,$TCAL$), $\vec{D}$ is defined explicitly in each event as,

$$\begin{aligned} D_x &= \frac{\sum_i (\pm 1) E_T^i \cos\phi_i}{\sum_i E_T^i} \\ D_y &= \frac{\sum_i (\pm 1) E_T^i \sin\phi_i}{\sum_i E_T^i} \\ \Psi_1[-\pi,\pi] &= \arctan(\frac{D_y}{D_x}) \end{aligned}$$

The summation index i goes through all cells within specific pseudo-rapidity window. With the assignment of $+1(-1)$ for forward(backward) cell and the use of E_T as the weighting factor, the experimentally defined $\vec{D}$ points to where most E_T is directed in the forward hemisphere. The randomness of the orientation of collisions should in principle leads to a flat azimuthal distribution of $\vec{D}$ in any oberserving window. However, some dead towers and wrong energy calibration might distort $\vec{D}$ to be not a $2D$ isotropic distribution around the origin in the directivity plane. We show in the following how to deal with this problem and construct event shape $\frac{dE_T}{d\varphi d\eta}$. All these procedures are done for the same event class which is characterized by centrality in our analysis.

1. Determine the center of the whole distribution (D_x^0, D_y^0) of the whole event sample, and define it as the new origin of the directivity distribution.

$$D^0_{x,y} = \frac{1}{N}\sum_{i=1}^{N} D_{x,y}$$

where N is total number of events in this event class.

$$D'_{x,y} = D_{x,y} - D^0_{x,y}$$

2. For each tower of $TCAL$ or $PCAL$, we get $\frac{dE_T}{d\varphi'}$ and $\frac{dN}{d\varphi'}$ event-averagely. Here φ' is the relative angle between the fixed geometrical azimuthal angle of the tower and reaction plane angle Ψ_1 which is measured by the corrected directivity $D'_{x,y}$ event by event. The reaction plane information used should be taken from the window independent of the cell, i.e. no possibility of shower sharing, to avoid the effect of autocorrelation.

$$\begin{aligned}
\Psi_1 &= \arctan\left(\frac{D'_y}{D'_x}\right) \\
\frac{dE_T}{d\varphi'} &= \frac{1}{N_0}\sum_{i=1}^{N_0} \frac{dE_T}{d\varphi'_i} \\
\frac{dN}{d\varphi'} &= \frac{1}{N_0}\sum_{i=1}^{N_0} \frac{dN}{d\varphi'_i} \\
\varphi'_i &= \phi - \Psi_1^i
\end{aligned}$$

where the i is the event index and ϕ is the fixed azimuthal angle of each cell in the lab system. The random distribution of Ψ_1^i will automatically fill the whole distribution over 2π.

3. If the phase space of the events, $\frac{dN}{d\varphi'}$, is not uniform over the phase space, we can re-normalize $\frac{dE_T}{d\varphi'}$ by dividing it with $\frac{dN}{d\varphi'}$ and get the average azimuthal distribution of E_T in one event. This step assumedly makes $\frac{dN}{d\varphi'}$ flat and circularize the distribution of $D'_{x,y}$. The essential condition of validating this flattening step is that there should be enough statistics in each bin of $\frac{dN}{d\varphi'}$. That means that the first step is quite necessary to make the distribution cover the whole range.

$$\langle \frac{dE_T}{d\varphi'} \rangle = \frac{dE_T}{d\varphi'} / \frac{dN}{d\varphi'}$$

4. To increase statistics, we group cells, after excluding the known dead or sick ones, into different pseudo-rapidity windows and construct $\frac{dE_T}{d\varphi d\eta}$ which is the event shape of E_T.

5. Now, for the event class of the same defined centrality and pseudo-rapidity bin(η), we perform Fourier analysis of $\frac{dE_T}{d\varphi'}$ and get $(\tilde{v_n}', \psi_n)$ representing anisotropic flow signals of transverse energy distribution.

$$\frac{dE_T}{d\varphi'} |_{\eta,centrality} = \frac{\langle E_T \rangle}{2\pi} + \frac{1}{\pi} \sum_{n=1}^{\infty} (a_n \cos(n\varphi') + b_n \sin(n\varphi'))$$

For each moment n,

$$\begin{aligned} \tilde{v_n}' &= \frac{\sqrt{a_n^2 + b_n^2}}{\langle E_T \rangle} \\ \psi_n &= \arctan(\frac{b_n}{a_n}) \\ sign(\tilde{v_n}') &\equiv sign(a_n) \end{aligned}$$

Because of the mirror symmetry of reaction plane, b_n should be equal to be zero theoretically and the nonzero-ness of it could be used as a estimate of error of a_n. The convention of the sign is positive for the forward direction(that of beam particle).

6. The azimuthal distribution $\frac{dE_T}{d\varphi'}$ is constructed with respect to the measured reaction plane Ψ_1 instead of the true one Ψ_R. So $\tilde{v_n}'$ needs to be corrected by the finite angular resolution of determining Ψ_1. How to get the correction factors $\langle\cos(n\Delta\Psi_1)\rangle$ of different $\tilde{v_n}$ will be discussed in the next section.

$$\tilde{v_n} = \frac{\tilde{v_n}'}{\langle\cos(n\Delta\Psi_1)\rangle}$$

3 Reaction Plane Resolution

As is discussed before, the reaction plane is defined as the plane spanned by the beam momentum and the impact parameter vector. The projection of it on the transverse plane specifies reaction plane angle Ψ_R. The existence of collective flow in the transverse direction make it possible to estimate Ψ_R event by event. In general, the estimation of Ψ_R in our experiment could be $n\Psi_n$.

$$\Psi_n = \arctan\left(\frac{\sum_i(\pm 1)E_T^i \sin\ n\phi_i}{\sum_i E_T^i} / \frac{\sum_i(\pm 1)E_T^i \cos\ n\phi_i}{\sum_i E_T^i}\right)$$

The reaction plane resolution is defined as correlation of measured reaction plane angle $n\Psi_n$ and the true one Ψ_R. It is mainly limited by the finite granuality and energy resolution of the towers used in the measurement and the magnitude of the flow signal appearing. Either wrong calibration or dead tower could also leads to worse resolution, but this source should be cured if the distribution of $n\Psi_n$ has been corrected to be uniform over 2π in our procedure. The distortion become more significant for $n\Psi_n$ of larger n. So we take the first moment Ψ_1 from $\vec{D}$(directivity) as our estimation.

The resolution of the nth moment of flow signal can be quantified as $\langle\cos\ n(\Psi_1 - \Psi_R)\rangle$. The bracket means the event averaged. The following discussion is for the first moment(n=1) only and could be extended to higher moment.

Any pseudo-rapidity segment of calorimeter which possesses 2π coverage over azimuthal angle could be used as an window to determine the reaction plane. In the approach in the ref [1] and after the flow signal $\tilde{v_1}$ and fluctuation σ be known, the resolution of reaction plane can be expressed analytically as [4]

$$\langle\cos(\Psi_1 - \Psi_R)\rangle = 2^{-3/2}\frac{\Gamma(1/2)}{\Gamma(1)}(\frac{\tilde{v_1}}{\sigma})\exp(-\frac{\tilde{v_1^2}}{2\sigma^2})\ {}_1F_1(3/2, 2, \frac{\tilde{v_1}^2}{2\sigma^2})$$

If three Ψ_1^i are determined in three independent windows(no other correlation except the directed flow signal) for the same event, the resolution could be known by calculating the correlation of Ψ_1^i [6].

$$\begin{aligned}\cos(\Psi_1^i - \Psi_1^j) &= \cos((\Psi_1^i - \Psi_R) - (\Psi_1^j - \Psi_R)) \\ &= \cos(\Psi_1^i - \Psi_R)\cos(\Psi_1^j - \Psi_R) + \sin(\Psi_1^i - \Psi_R)\sin(\Psi_1^j - \Psi_R)\end{aligned}$$

Take the event average of both sides and assume the only correlation is between Ψ_1 and Ψ_R, then

$$
\begin{aligned}
\langle\cos(\Psi_1^i-\Psi_1^j)\rangle &= \langle\cos(\Psi_1^i-\Psi_R)\cos(\Psi_1^j-\Psi_R)\rangle+\langle\sin(\Psi_1^i-\Psi_R)\sin(\Psi_1^j-\Psi_R)\rangle \\
&= \langle\cos(\Psi_1^i-\Psi_R)\rangle\langle\cos(\Psi_1^j-\Psi_R)\rangle+\langle\sin(\Psi_1^i-\Psi_R)\rangle\langle\sin(\Psi_1^j-\Psi_R)\rangle \\
&= \langle\cos(\Psi_1^i-\Psi_R)\rangle\langle\cos(\Psi_1^j-\Psi_R)\rangle
\end{aligned}
$$

The second term on the right hand side vanishes because of the symmetry of our colliding system with respect to reaction plane.

After the correlation between any two windows are known, the resolution of one specific window is expressed as

$$
\mid \langle\cos(\Psi_1^i-\Psi_R)\rangle \mid = \sqrt{\frac{\langle\cos(\Psi_1^i-\Psi_1^j)\rangle\langle\cos(\Psi_1^i-\Psi_1^k)\rangle}{\langle\cos(\Psi_1^j-\Psi_1^k)\rangle}}
$$

There exists a question: How will the non-uniformity of distribution of reaction plane in each window affect the correlation value ? To tackle it, we compare the values of correlation between different window in two ways. The first is the direct calculation of $\langle\cos(\Psi_1^i-\Psi_1^j)\rangle$ event by event. In the other one, we define normalized function of angle correlation as

$$
\begin{aligned}
\frac{dP}{d\Delta\Psi_1^{ij}} &= \frac{dN}{\Delta\Psi_1^{ij}}\,\Big|_{same\ event} \Big/ \frac{dN}{\Delta\Psi_1^{ij}}\,\Big|_{mixed\ event} \\
\Delta\Psi_1^{ij} &= \Psi_1^i-\Psi_1^j
\end{aligned}
$$

The "mixed event" label means that the Ψ_1^i , Ψ_1^j are randomly selected from events of the same event class. The entry of the denominator is taken as much as possible to define a smooth background shape. Then the resolution is calculated by mean of this probability function.

$$\langle \cos(\Psi_1^i - \Psi_1^j) \rangle = (\int \frac{dP}{d\Delta\Psi_1^{ij}} \cos(\Psi_1^i - \Psi_1^j) d\Delta\Psi_1^{ij}) / (\int \frac{dP}{d\Delta\Psi_1^{ij}} d\Delta\Psi_1^{ij})$$

So we expect the effect of the non-uniformity of individual Ψ_1^i, Ψ_1^j on the $\langle \cos(\Psi_1^i - \Psi_1^j) \rangle$ should be straightened out. Fig. 1 illustrates the whole procedures.

4 Results of Analysis

First the resolution of reaction plane in each defined pseudo-rapidity window is determined. Then we show the Fourier moment of E_T flow which characterizes the anisotropy of the event shape as the function of pseudo-rapidity η and centrality cut $PCAL\ E_T$. In the end of this section, we make comparison with different model prediction and the results of ref [1] in larger pseudo-rapidity bins.

4.1 Reaction Plane Resolution

According to the convention in the ref [6], we define four independent pseudo-rapidity windows. They are divisions in the angle dimension instead of the depth one.

The event-averaged values of correlation of reaction plane angle determined in different windows $\langle \cos(\Psi_1^i - \Psi_1^j) \rangle$ and $\langle \cos\ 2(\Psi_1^i - \Psi_1^j) \rangle$ are shown in Fig. 2 and 3 as functions of centrality. The reaction plane angles in the backward pseudo-rapidity windows $TCAL$,$PCAL\,1$ are consistently

Table 1: Definition of windows in the pseudo-rapidity

Windows	η
TCAL	[-0.5, 0.7]
PCAL1	[0.8, 1.4]
PCAL2	[2.0, 2.7]
PCAL3	[2.7, 4.5]

antiparrellel to those in the forward windows $PCAL2$,$PCAL3$ and the anti-correlation become most evident in the mid-centrality where there exists strongest directed flow signal and best reaction plane resolution. The unexpected anti-correlation of $TCAL$ and $PCAL1$ in the low centrality is probably the result of upstream interaction around the target. Then we determine the resolution correction for first moment $\langle\cos(\Psi_1^i - \Psi_R)\rangle$(or the second moment $\langle\cos 2(\Psi_1^i - \Psi_R)\rangle$) by using it as the fit parameter in the simultaneous fitting of the six correlation values between four windows(Fig. 2 3). The results are shown in the Fig. 4(Fig. 5). In average, we have the resolution about 50 degree for the first moment and 80 degree for the second moment.

4.2 Flow Signal

In the Fig. 6, the event shape of E_T production with respect to the reaction plane are displayed from peripheral to central events. The anisotropy is most evident in the mid-centrality and the direction of the most transverse energy production shifts from 0 degree in the forward η to 180 degree in the backward η. This back-to-back correlation in the forward and backward η is just the characteristic of directed flow.The shortage of E_T observed in the backward direction is due to the energy leakage on $TCAL$ calorimeter.

The directed flow signal is extracted by either calculation of Fourier moments or fit the event shape with Fourier function and shown in the fig. 7 8. The different symbols represent different input of reaction plane information. The autocorrelation effect is quite obvious that the flow signal get false enhancement if the reaction plane is determined within the same pseudo-rapidity region. Remove the data point where there is possibility of autocorrellation and correct the value by reaction plane resolution(Fig. 9 10). The reliability of our method is tested to be good because close flow signals appears after resolution correction even though the resolution corrections could be different by factor of 2. The $PCAL$ 1 shows a odd behavior and the guessed reason for this is because it sits in the mid-rapidity where the first moment flow signal as used to determine the reaction plane is weakest and the possible appearance of second moment might even cause distortion. So we show the consistent results in all region without utilizing $PCAL$ 1 in the fig. 11 12.

For the first moment, the flow signal becomes strong form peripheral to mid-centrality and diminishes gradually towards higher centrality. Different from the charged multiplicity flow signal(ref [6]), the transverse energy signals are pretty asymmetric in the forward and backward regions. This could be the combining results of pseudo-rapidity distribution of nucleon and pion and the carried flow signal. We could try to distengle them with some assumption in the following subsection. There is no evident second moment flow signal.

As a check up of the analysis, we take three large pseudo-rapidity windows in the ref [1] and the comparison agrees well except for the middle window(Fig. 15)

4.3 Model Comparison

The prediction from $RQMD$ cascade mode folding in the detector effect by GEANT simulation is shown in Fig. 13 14 and under-predict our observation by 20%. After turning on the mean field mechanism, the repulsive potential is expected to increase the prediction([7]). As for the hydro-dynamical model, it is not clear(??).

4.4 Distengle Nucleon and Pion

The energy deposited in the calorimeters mainly comes from nucleon and pion. Without direct particle identification, we propose the following way to distengle nucleon pion flow signal.

Formulation:

With each η slice for specific event class, the E_T measurement shows

$$\begin{aligned}
\frac{dE_T}{d\phi} &= \langle E_T \rangle (1 + 2\tilde{v_1}^{E_T} \cos\phi) \\
&= \frac{dE_T}{d\phi} |_N + \frac{dE_T}{d\phi} |_\pi \\
&= \langle E_T^N \rangle (1 + 2\tilde{v_1}^{E_T,N} \cos\phi) + \langle E_T^\pi \rangle (1 + 2\tilde{v_1}^{E_T,\pi} \cos\phi) \\
&= (\langle E_T^N \rangle + \langle E_T^\pi \rangle)(1 + 2\frac{\langle E_T^N \rangle \tilde{v_1}^{E_T,N} + \langle E_T^\pi \rangle \tilde{v_1}^{E_T,\pi}}{\langle E_T^N \rangle + \langle E_T^\pi \rangle} \cos\phi)
\end{aligned}$$

and the measurement of charged multiplicity shows

$$\begin{aligned}
\frac{dM}{d\phi} &= \langle M\rangle(1+2\tilde{v_1}^{M}\cos\phi) \\
&= \frac{dM}{d\phi}\mid_{p}+\frac{dM}{d\phi}\mid_{\pi+-} \\
&= \langle M^{p}\rangle(1+2\tilde{v_1}^{M,p}\cos\phi)+\langle M^{\pi+-}\rangle(1+2\tilde{v_1}^{M,\pi+-}\cos\phi) \\
&= (\langle M^{p}\rangle+\langle M^{\pi+-}\rangle)(1+2\frac{\langle M^{p}\rangle\tilde{v_1}^{M,p}+\langle M^{\pi+-}\rangle\tilde{v_1}^{M,\pi+-}}{\langle M^{p}\rangle+\langle M^{\pi+-}\rangle}\cos\phi)
\end{aligned}$$

So,

$$\begin{aligned}
\tilde{v_1}^{E_T} &= \frac{\langle E_T^N\rangle\tilde{v_1}^{E_T,N}+\langle E_T^\pi\rangle\tilde{v_1}^{E_T,\pi}}{\langle E_T^N\rangle+\langle E_T^\pi\rangle} \\
&= a_1\tilde{v_1}^{E_T,N}+a_2\tilde{v_1}^{E_T,\pi} \\
\tilde{v_1}^{M} &= \frac{\langle M^{p}\rangle\tilde{v_1}^{M,p}+\langle M^{\pi+-}\rangle\tilde{v_1}^{M,\pi+-}}{\langle M^{p}\rangle+\langle M^{\pi+-}\rangle} \\
&= b_1\tilde{v_1}^{M,p}+a_2\tilde{v_1}^{E_T,\pi+-}
\end{aligned}$$

Folding into more informations and making some assumption,

- $a_1, a_2(b_1, b_2)$ are the separate ratios of$\langle E_T\rangle$(charged multiplicity) for nucleon and pion of the total $\langle E_T\rangle$(charged multiplicity). They can be known by assuming a thermal system of nucleon and pion and folding into isospin symmetry, the determined inverse temperature from particle spectrum and rapidity distribution and calculating the ratios in the pseudo-rapidity coordinate.
- As for the carried flow signal, proton behaves similarly like neutron and so as charged pion do like neutral one. So $\tilde{v_1}^{E_T,p}=\tilde{v_1}^{E_T,N}$ and $\tilde{v_1}^{E_T,\pi}=\tilde{v_1}^{E_T,\pi+-}$.

- Another essential assumption is that

$$\tilde{v_1}^{p} = \tilde{v_1}^{E_T,p} = \tilde{v_1}^{M,p}$$

,and

$$\tilde{v_1}^{\pi+-} = \tilde{v_1}^{E_T,\pi+-} = \tilde{v_1}^{M,\pi+-}$$

This basically assumes that the E_T/M is isotropic azimuthally. The observed anisotropy in the E_T shape is caused by anisotropy of the multiplicity of particles.

With the input of $\tilde{v_1}^{E_T}$,$\tilde{v_1}^{M}$ which are experimental measured, the $\tilde{v_1}^{p}$,$\tilde{v_1}^{\pi+-}$ can be solved.

Unfortunately, the last assumption is checked to be invalid for nucleon in the $RQMD$ produced event shape. Shown in the fig. 16, the solid line represent the E_T/M for nucleon reveals notable baring anisotropy from backward to forward η while the dash line for pion is more or less flat.

5 Summary

References

[1] J.Barrette, E877 Collaboration, Phys.Rev.Lett. **70** (1993) 2996.

[2] S.Voloshin, Y.Zhang, *hep-ph/9407282* (July 1994)

[3] S.Voloshin, *E877 Note#PITT-95-001*

[4] W.C.Chang, *E877 Note#SUNYSB-CHANG-95-001*

[5] Y.Zhang, private communication

[6] S.Voloshin, *E877 Note#PITT-95-005*

[7] H.Sorge, private communication

[8] Y.Zhang, PhD dissertation

Figure 1: The rows from top to bottom (1-6)are for correlation of $[TCAL, PCAL1]$, $[TCAL, PCAL2]$, $[TCAL, PCAL3]$, $[PCAL1, PCAL2]$, $[PCAL1, PCAL3]$, $[PCAL2, PCAL3]$(defined in the text). The columns from left to right(a-e) correspond to $\frac{dN}{\Delta\Psi_1^{ij}}\ |_{same;event}$, $\frac{dN}{\Delta\Psi_1^{ij}}\ |_{mixed;event}$, $\frac{dP}{d\Delta\Psi_1^{ij}}$, $\frac{dP}{d\cos\Delta\Psi_1^{ij}}$, $\frac{dP}{d\cos;2\Delta\Psi_1^{ij}}$

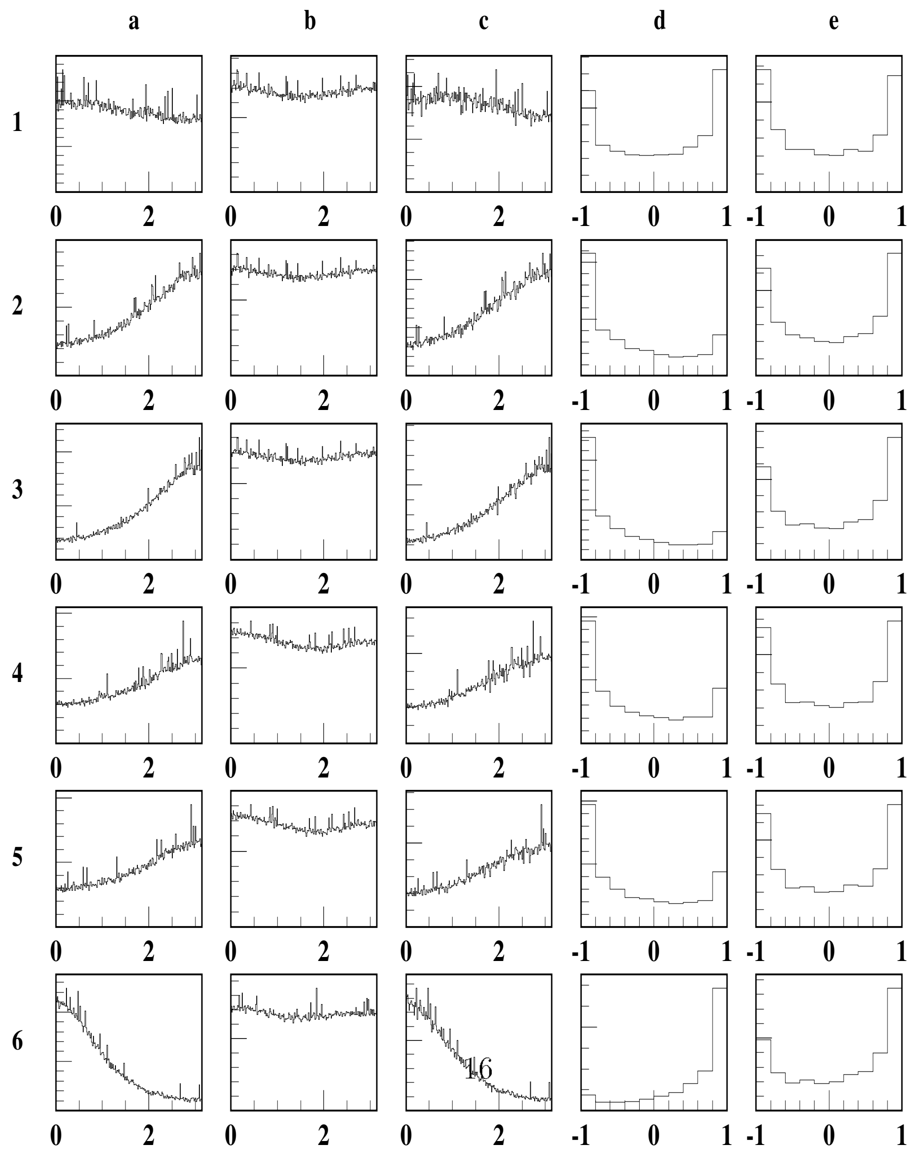

Figure 2: $\langle\cos(\Psi_1^i - \Psi_1^j)\rangle$ as the function of centrality

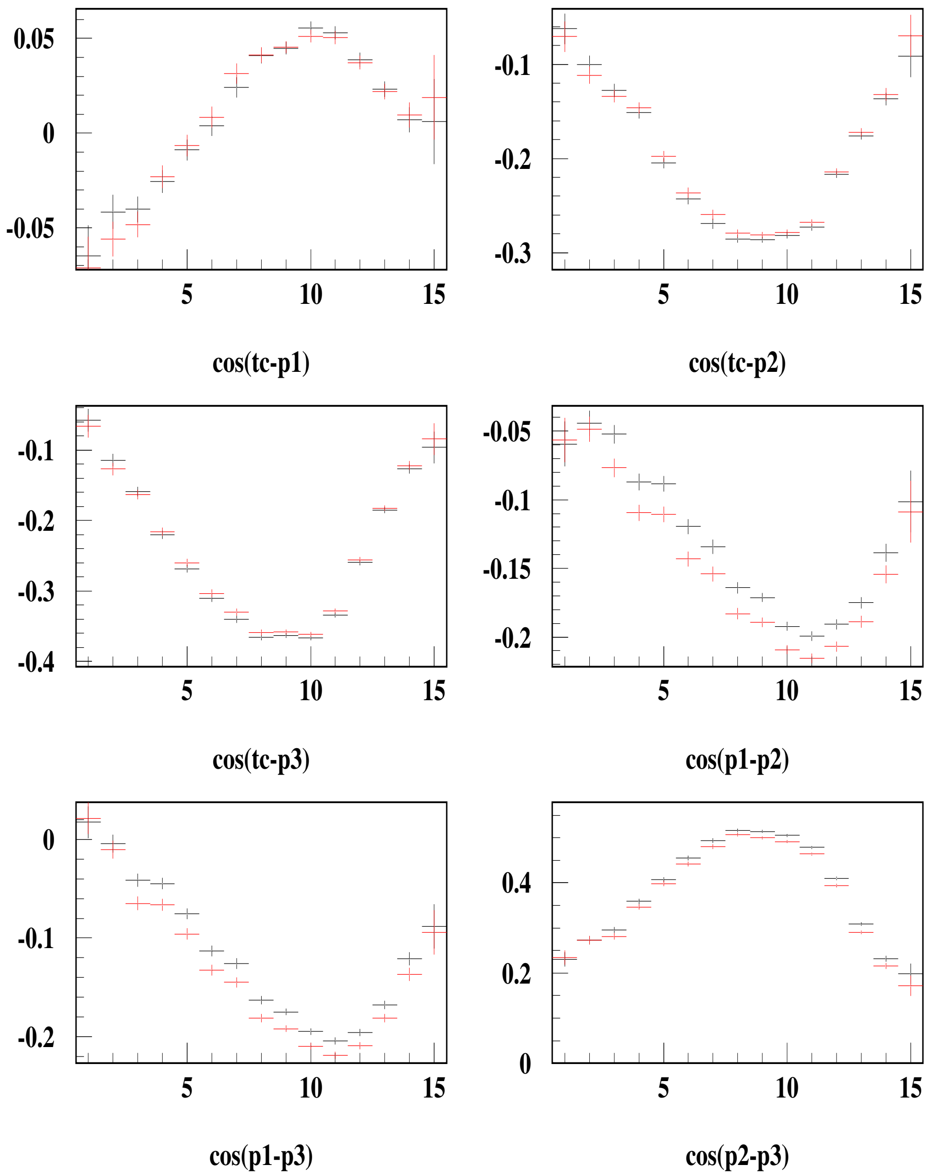

Figure 3: $\langle \cos ; 2(\Psi_1^i - \Psi_1^j) \rangle$ as the function of centrality

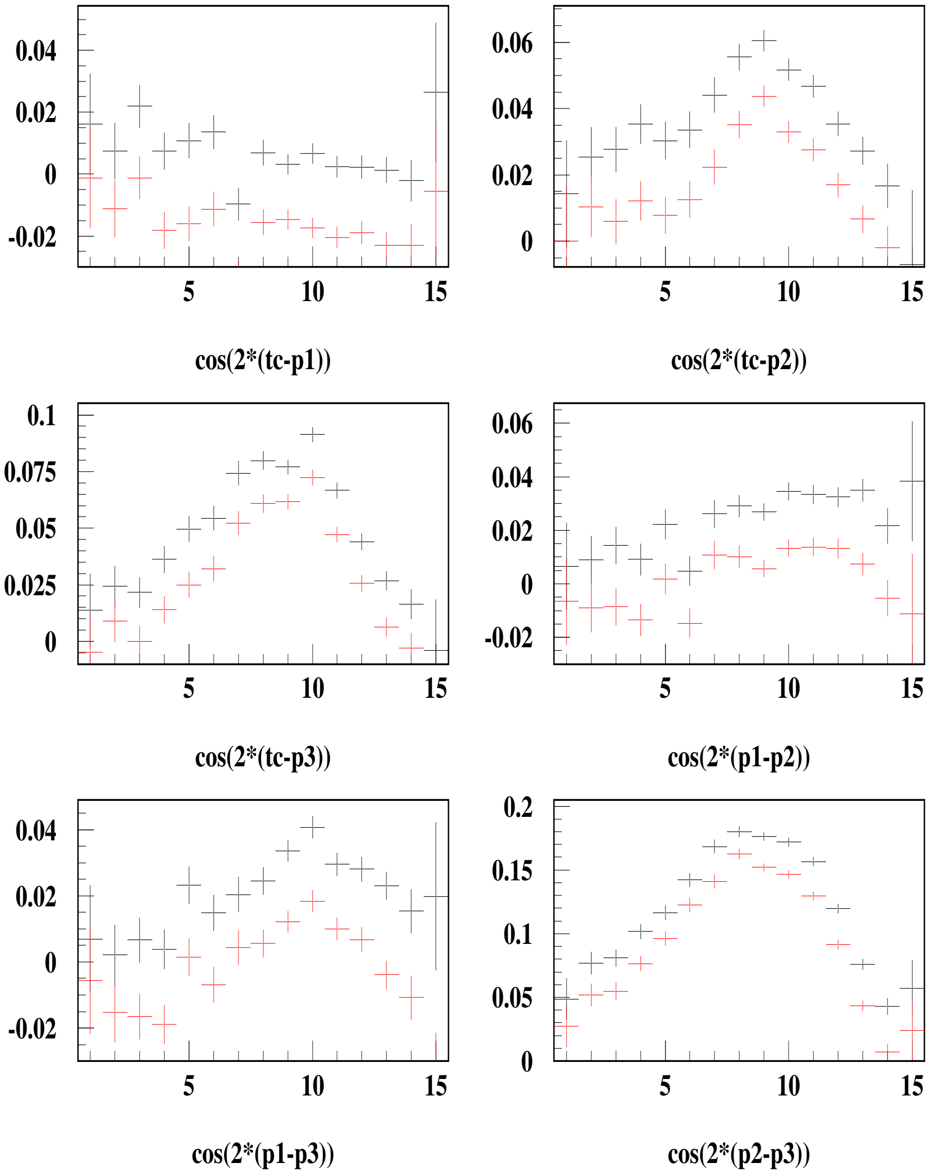

Figure 4: $\langle\cos(\Psi_1^i - \Psi_R)\rangle$

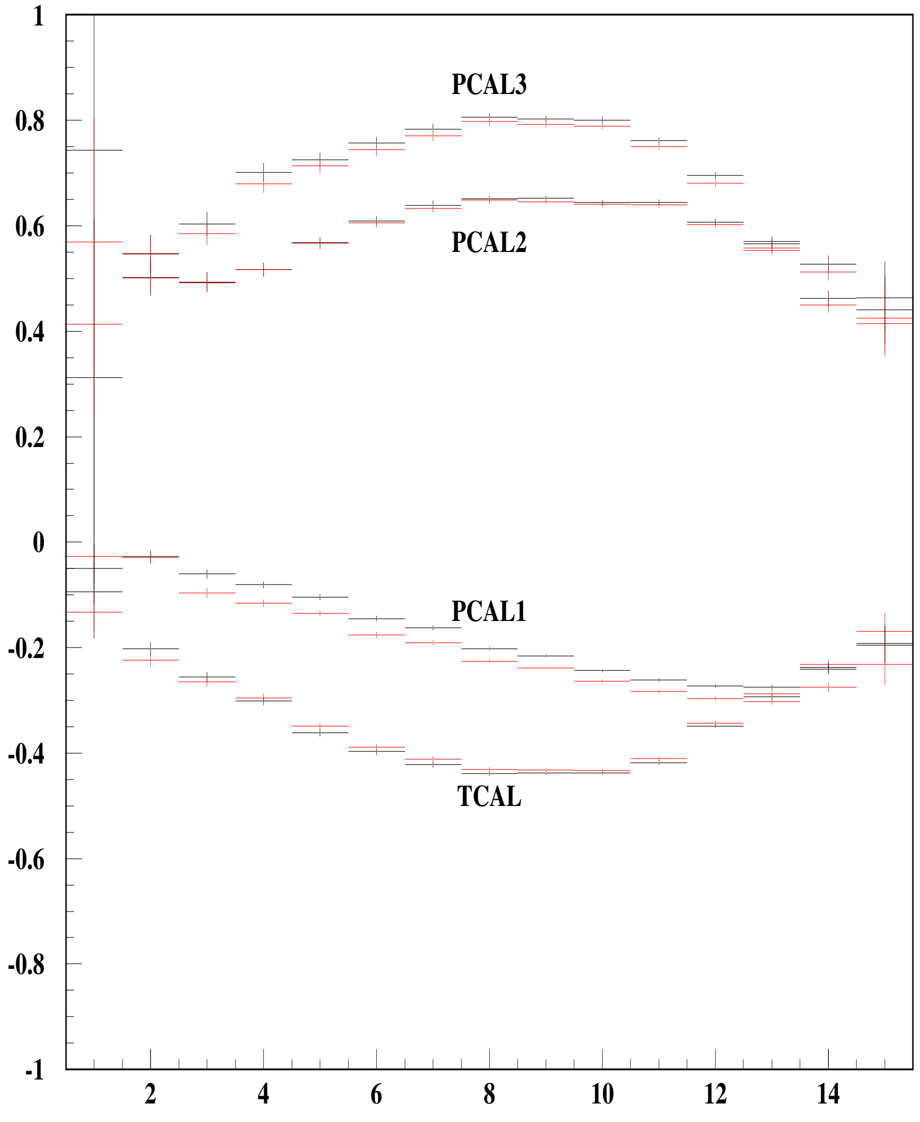

Figure 5: $\langle \cos 2(\Psi_1^i - \Psi_R) \rangle$

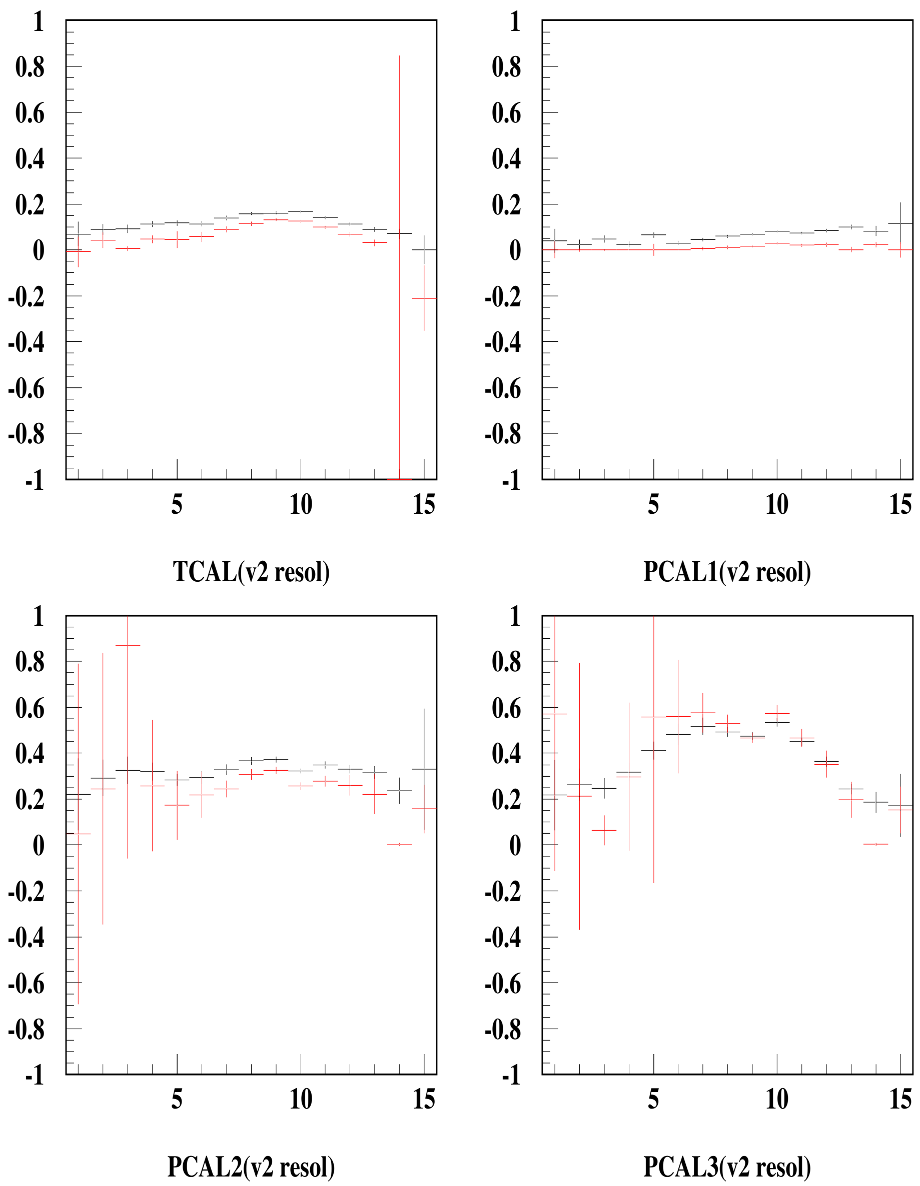

Figure 6: $dE_T/d\phi' d\eta$ for different centrality

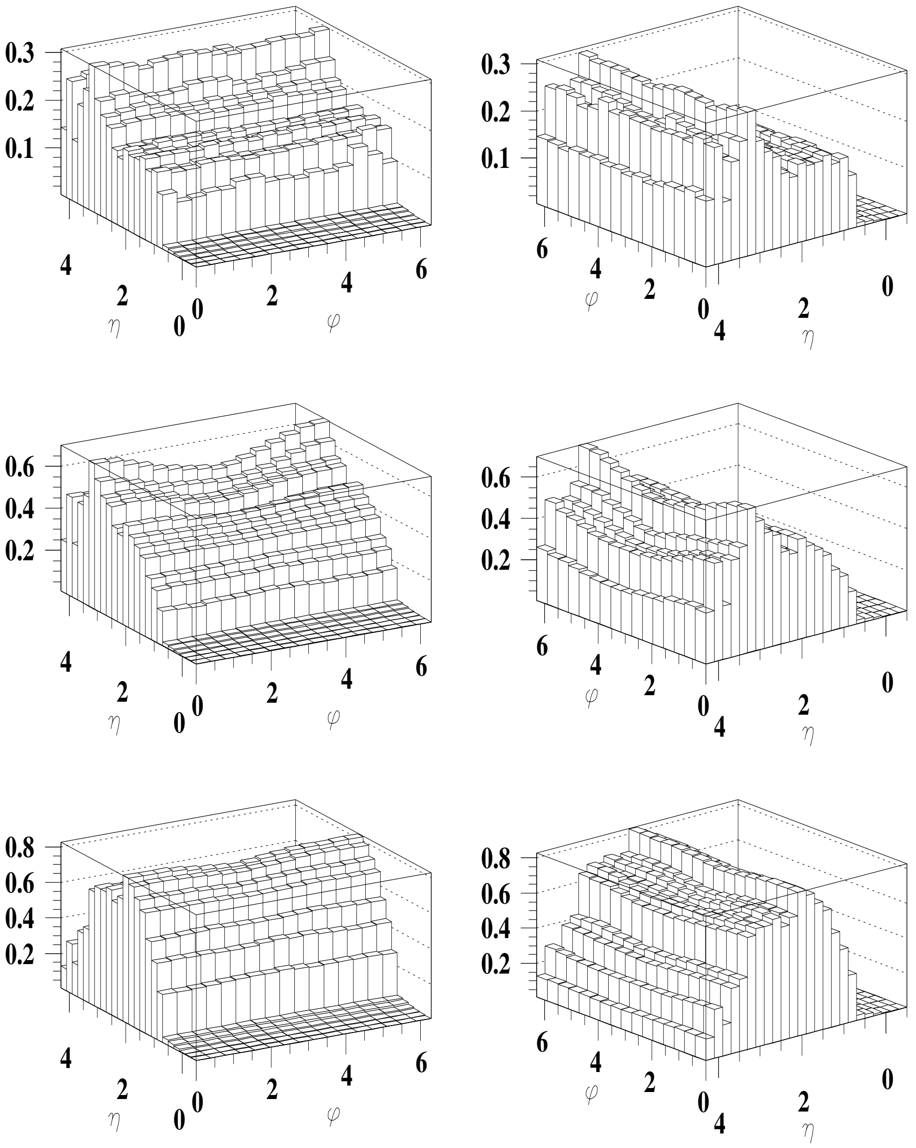

Figure 7: $\tilde{v}_1'$(before correction) as a function of η for different centrality. $\circ$: $TCAL$, $\square$: $PCAL\,1$, $\triangle$: $PCAL\,2$, $\diamondsuit$: $PCAL\,3$

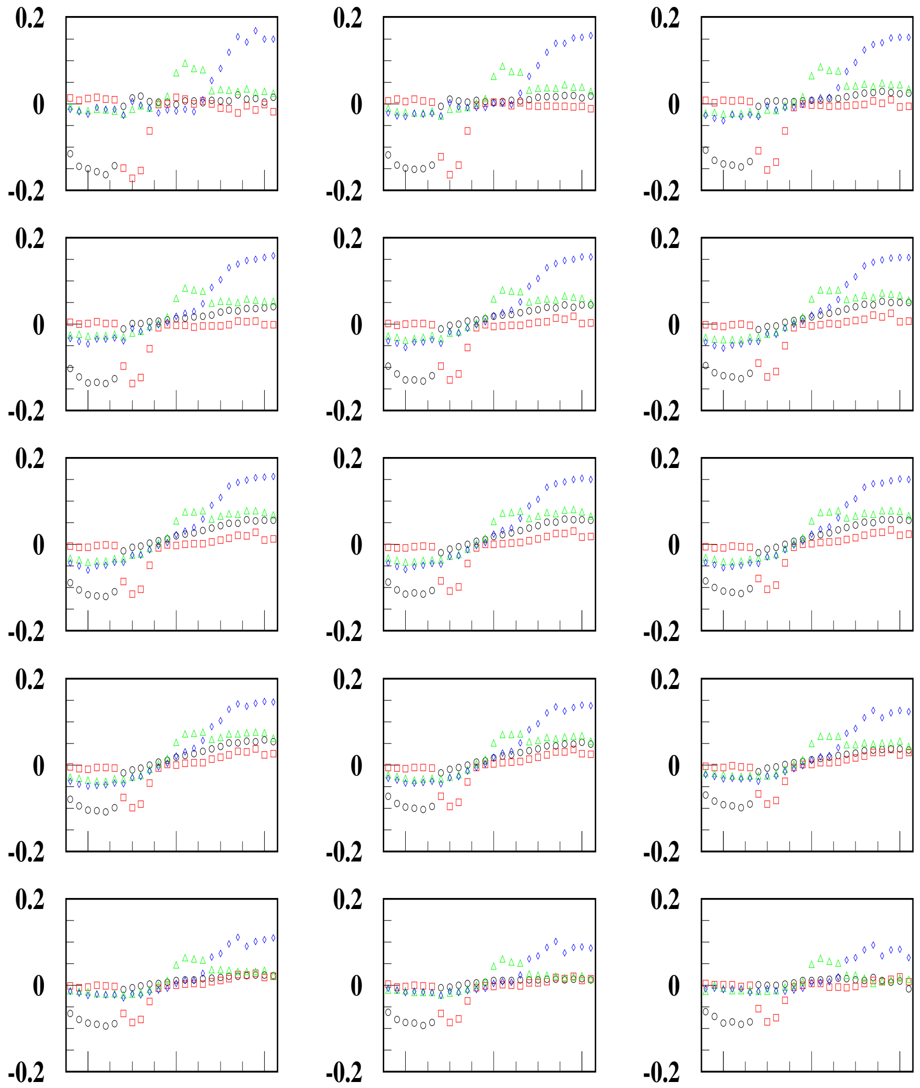

Figure 8: $\tilde{v_2'}$(before correction) as a function of η for different centrality. $\circ$: $TCAL$, $\square$: $PCAL\,1$, $\triangle$: $PCAL\,2$, $\diamondsuit$: $PCAL\,3$

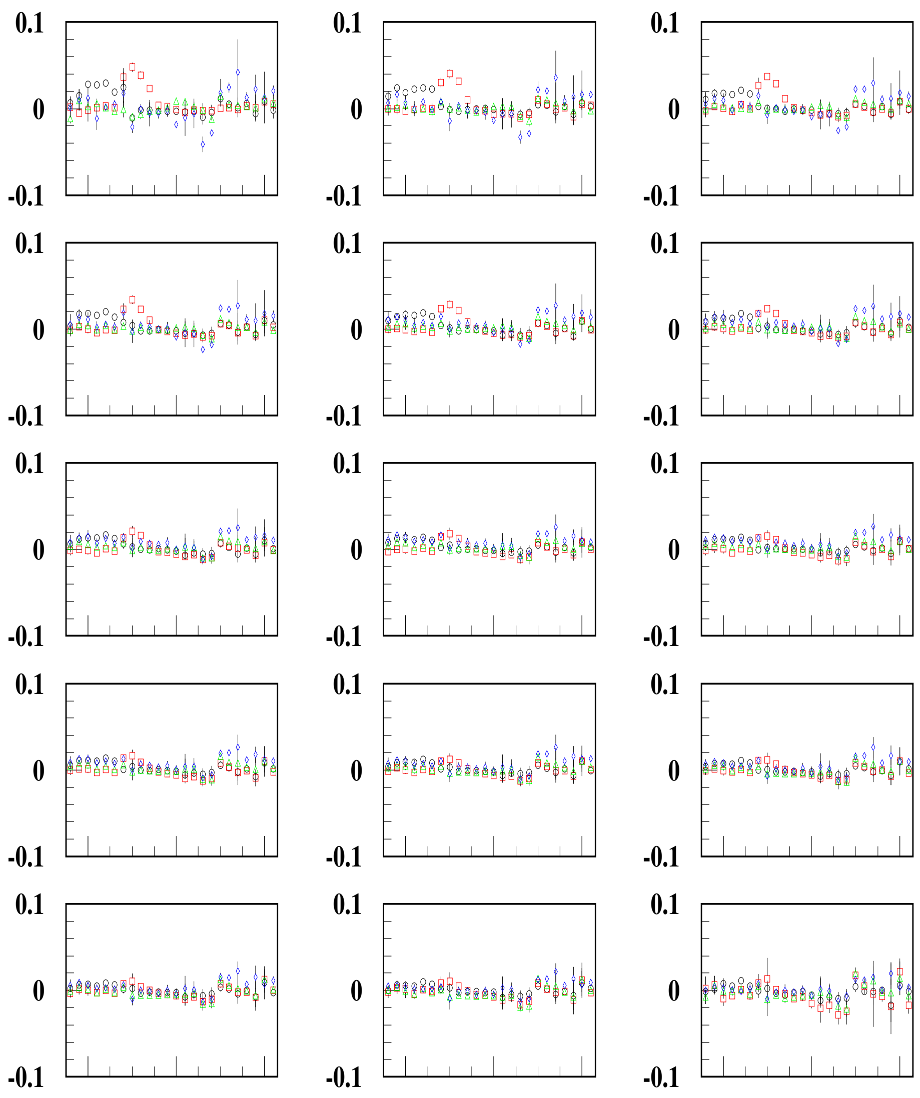

Figure 9: $\tilde{v}_1$(after correction) as a function of η for different centrality. $\circ$: $TCAL$, $\square$: $PCAL\,1$, $\triangle$: $PCAL\,2$, $\diamondsuit$: $PCAL\,3$

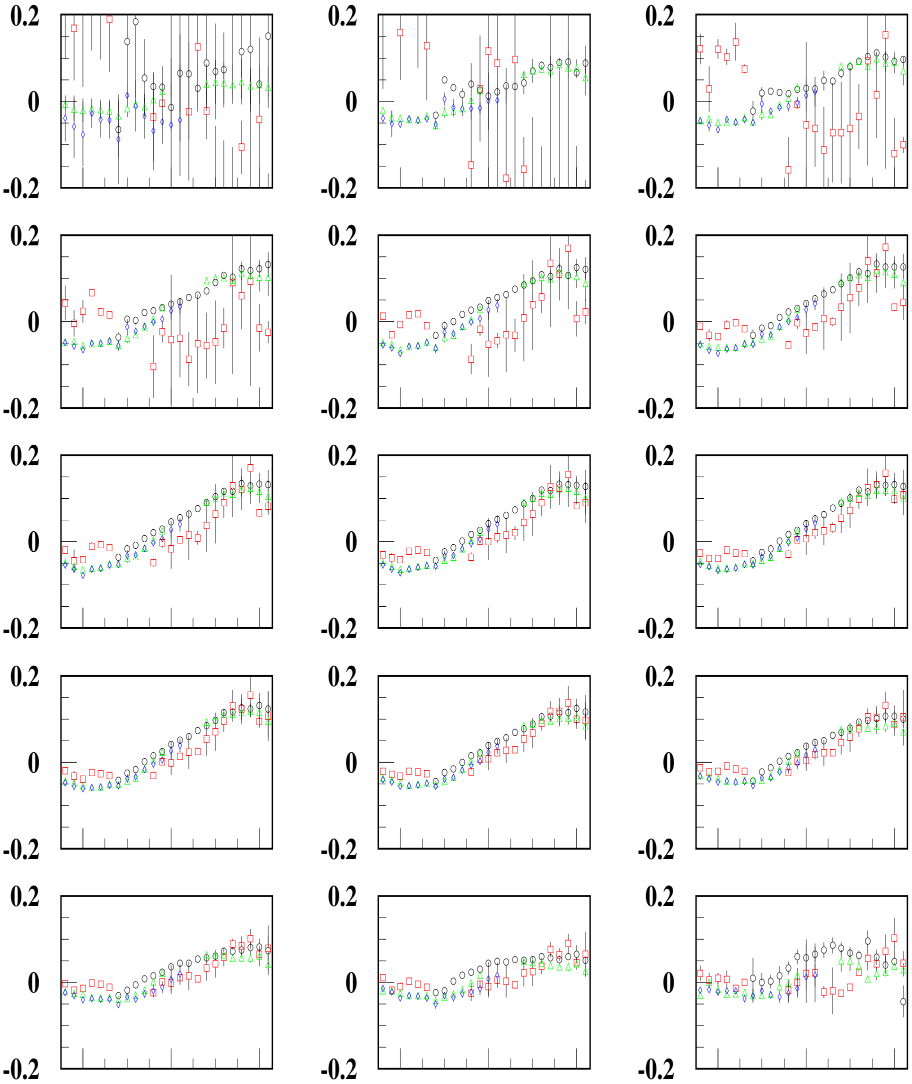

Figure 10: $\tilde{v_2}$(after correction) as a function of η for different centrality. $\circ$: $TCAL$, $\Box$: $PCAL\,1$, $\triangle$: $PCAL\,2$, $\diamondsuit$: $PCAL\,3$

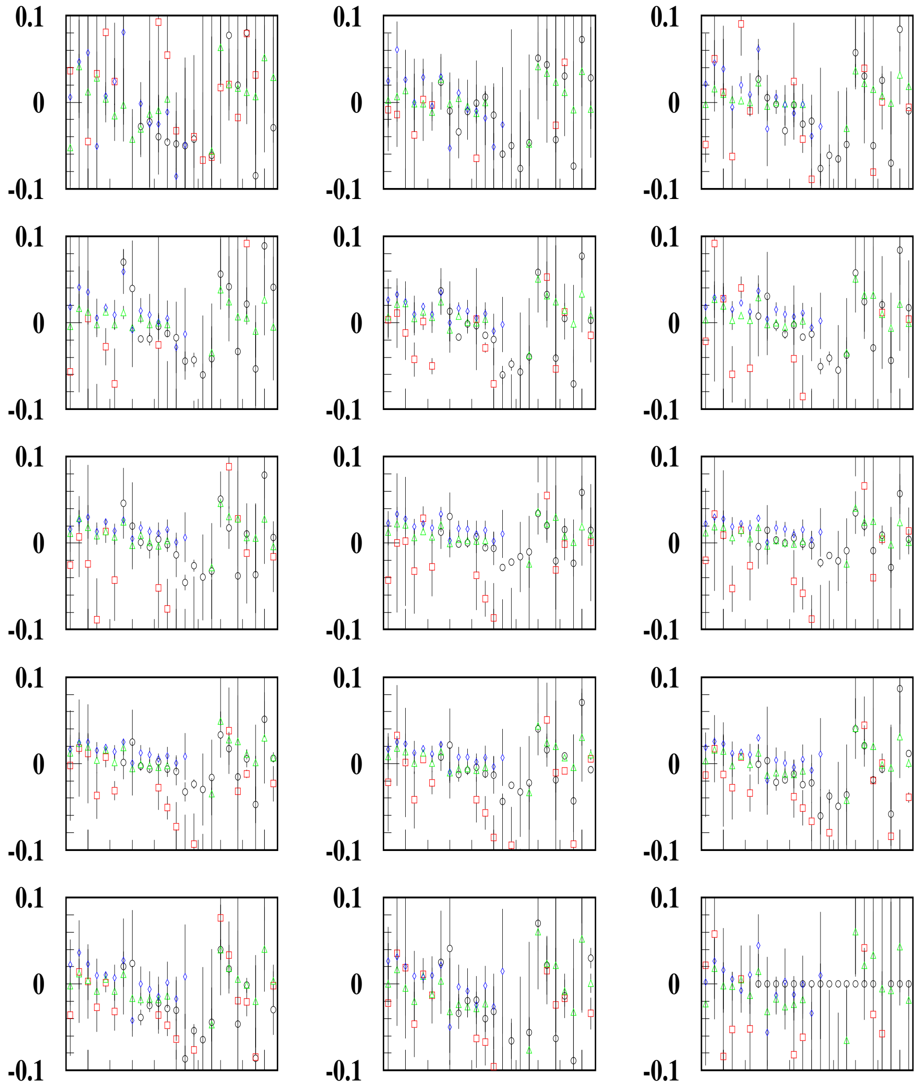

Figure 11: $\tilde{v}_1$ as a function of η for different centrality. $\circ$: $TCAL$, $\Box$: $PCAL\,1$, $\triangle$: $PCAL\,2$, $\diamondsuit$: $PCAL\,3$

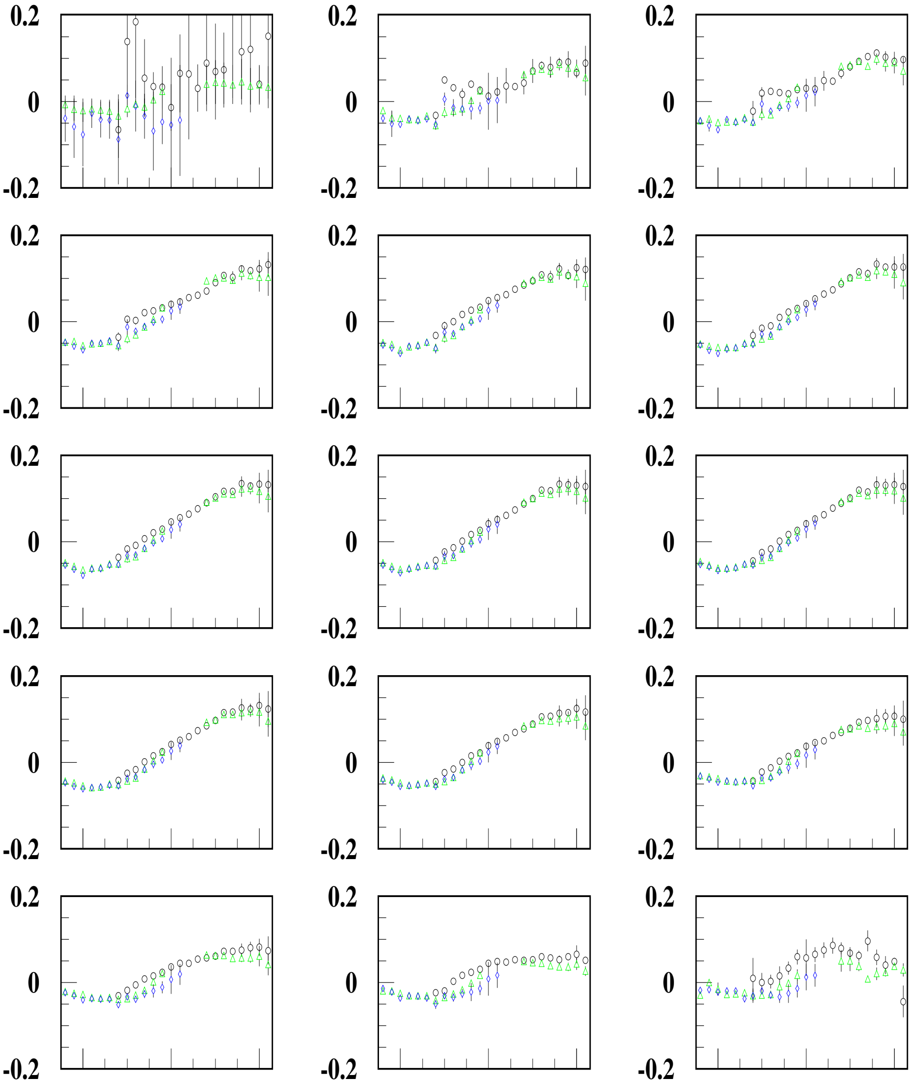

Figure 12: $\tilde{v}_2$ as a function of η for different centrality. $\circ$: $TCAL$, $\Box$: $PCAL\,1$, $\triangle$: $PCAL\,2$, $\diamondsuit$: $PCAL\,3$

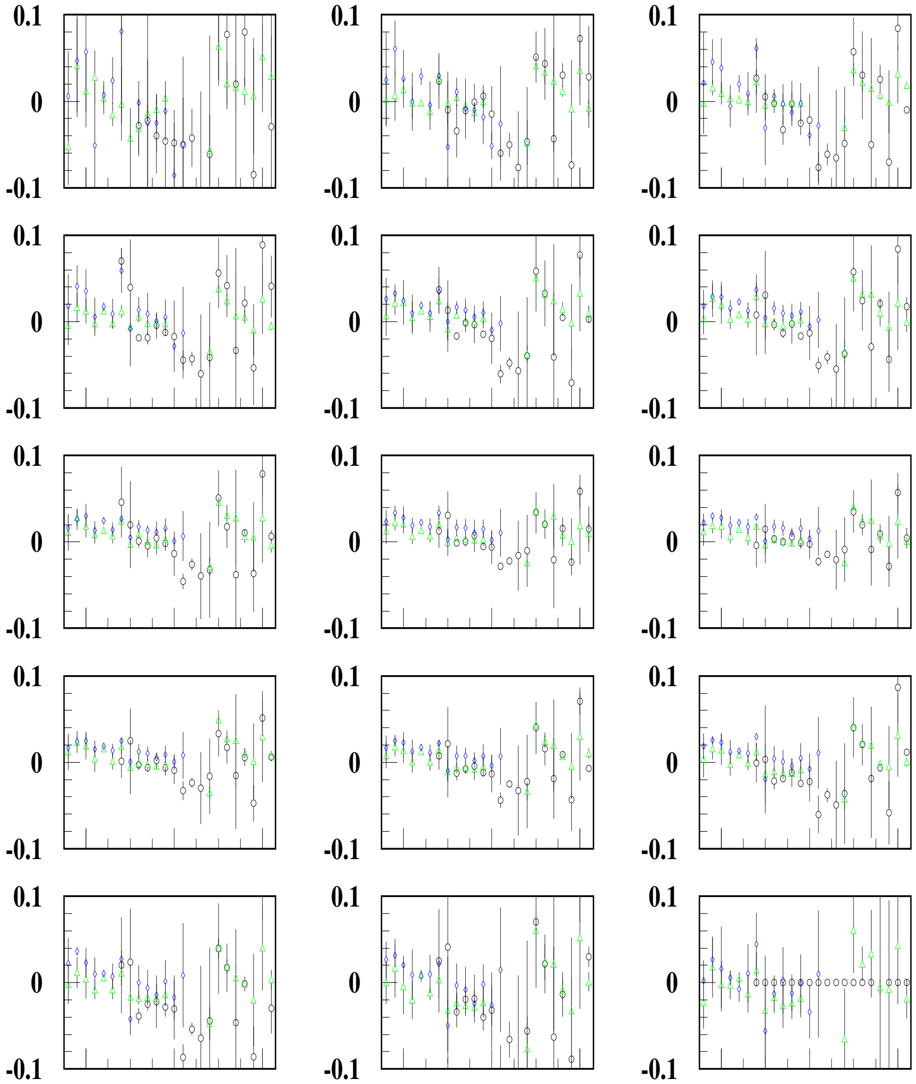

Figure 13: RQMD $\tilde{v}_1$ as a function of η for different centrality

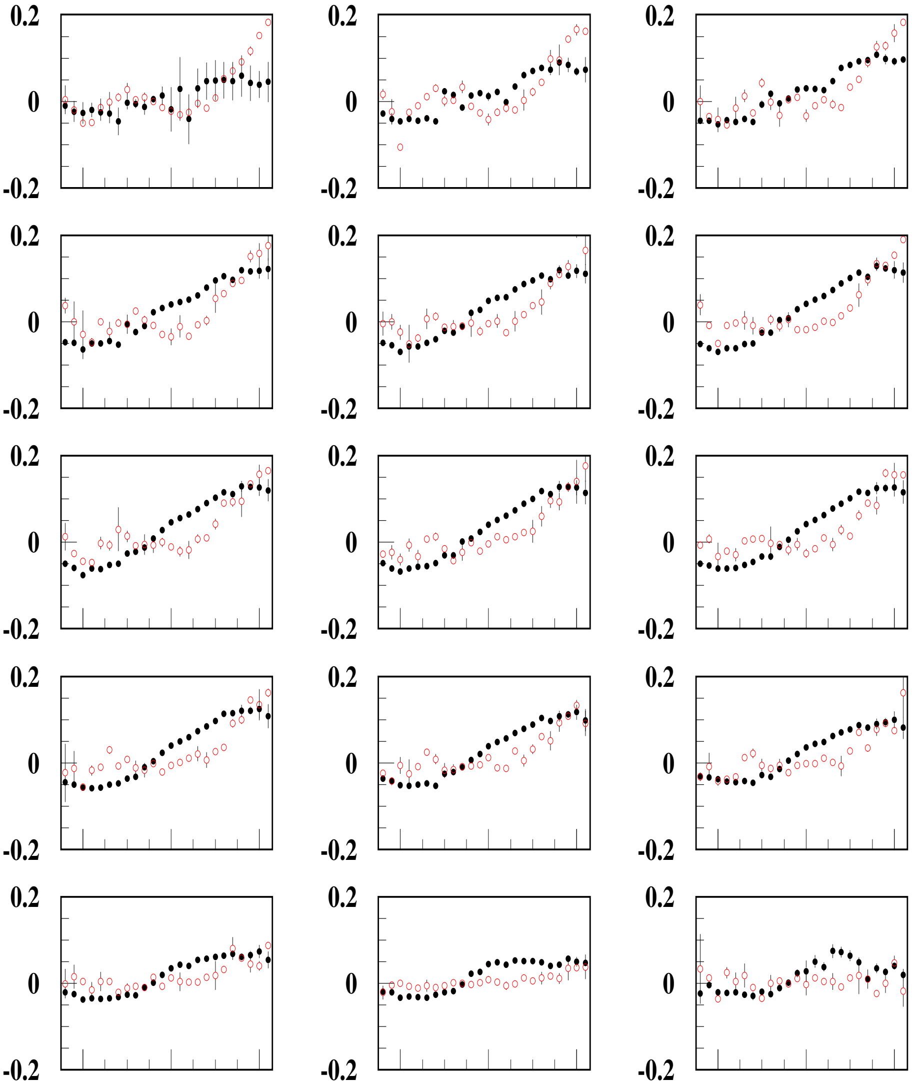

Figure 14: RQMD $\tilde{v}_2$ as a function of η for different centrality.

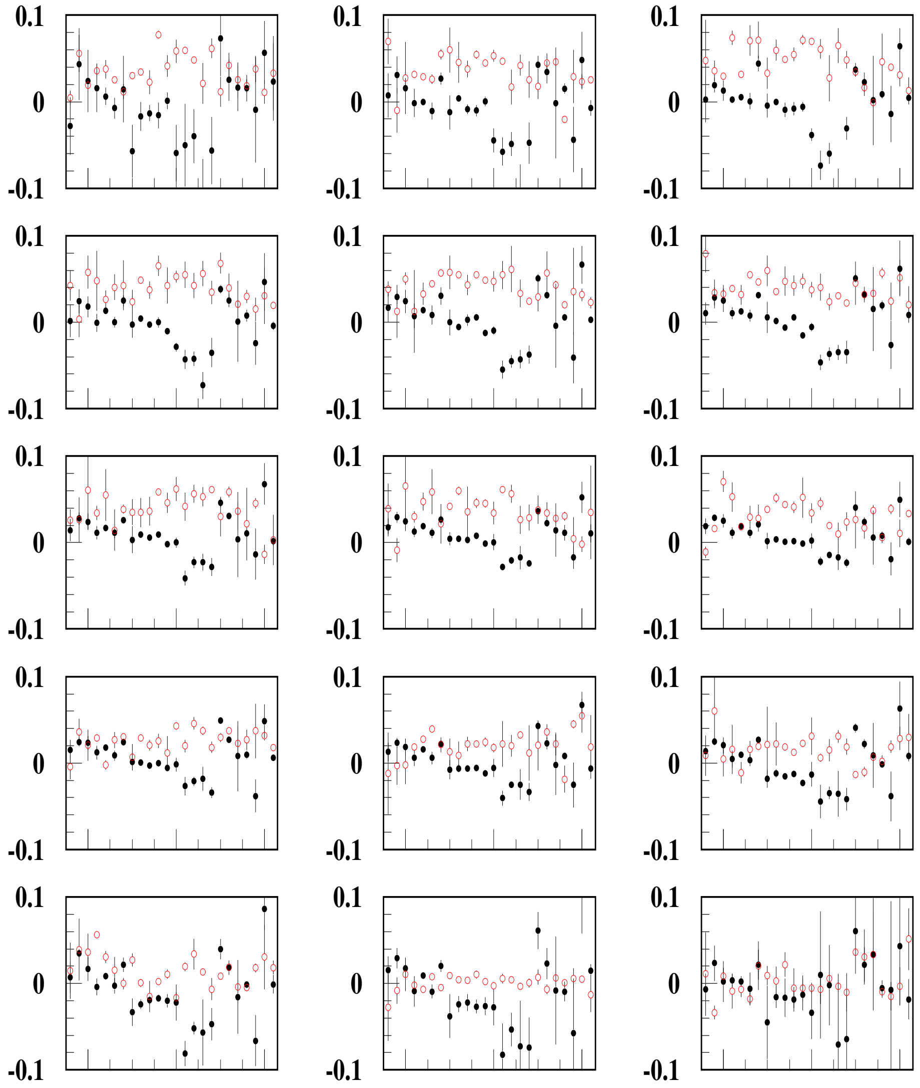

Figure 15: Comparison with Ref [1]

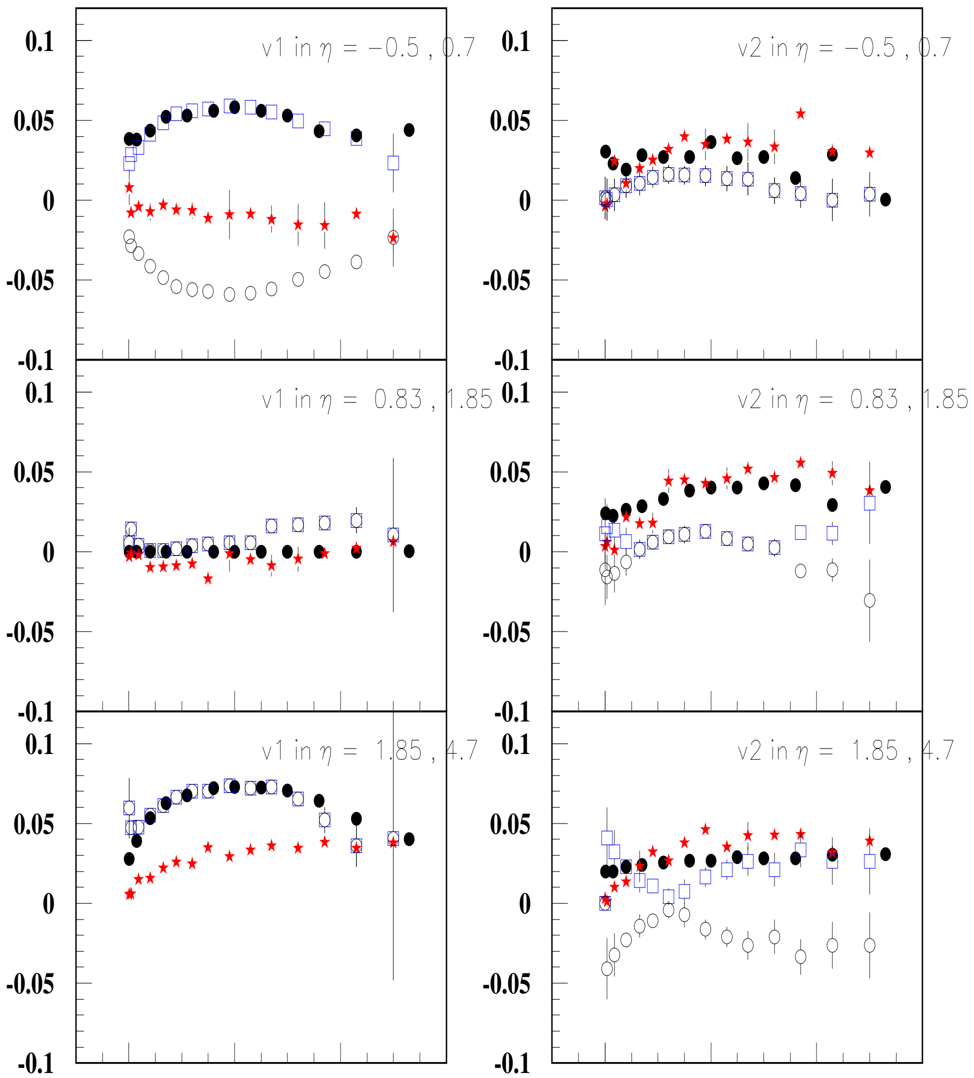

Figure 16: The azimuthal distributuion E_T/M in $RQMD$ model. The solid line is nucleon and the dash one is pion.